Roco kinase structures give insights into the mechanism of Parkinson disease-related leucine-rich-repeat kinase 2 mutations

Gilsbach, Bernd K.; Ho, Franz Y.; Vetter, Ingrid R.; van Haastert, Peter J. M.; Wittinghofer, Alfred; Kortholt, Arjan

Published in:
Proceedings of the National Academy of Sciences of the United States of America

DOI:
10.1073/pnas.1203223109

Publication date:
2012

Supporting Information

Gilsbach et al. 10.1073/pnas.1203223109

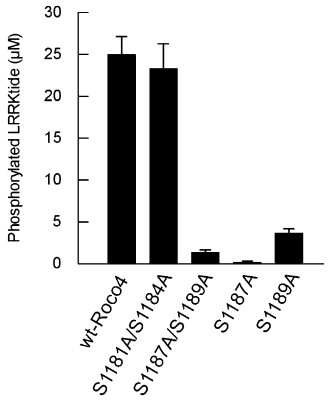

Fig. S1. Kinase activity of wild-type and activation loop-mutant Roco4 as indicated. Roco4-catalyzed phosphorylation of LRRKtide was measured by incubating 3 μM Roco with 150 μM LRRKtide and 25 μM radioactive ATP for 30 min. Data shown are the mean and SD of at least four independent experiments.

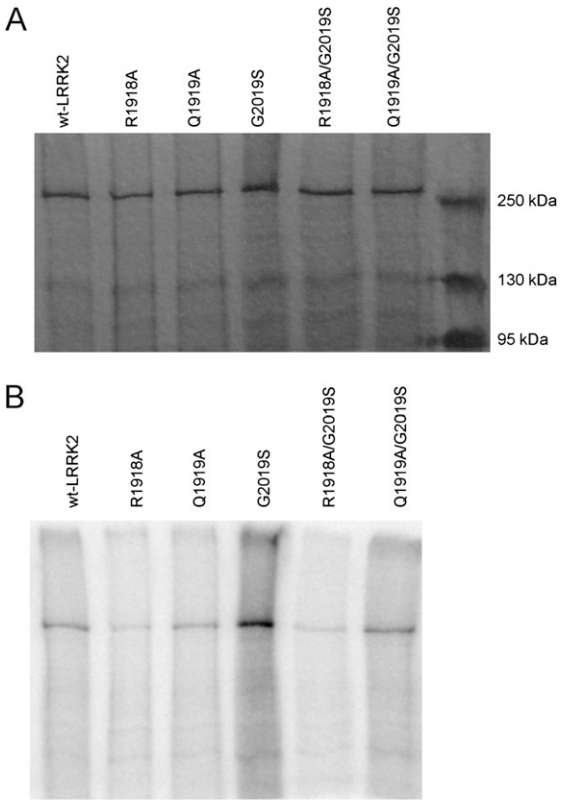

Fig. S2. Autophosphorylation of LRRK2. HEK293T cells overexpressing N-terminally Flag-tagged LRRK2 were lysed, and then Flag-LRRK2 were collected by immunoprecipitation using anti-Flag (M5) antibody (Sigma) overnight. (*A*) Silver-stained gel. Samples were taken, mixed with Laemmli buffer, and run on SDS/PAGE to normalize protein input. (*B*) Autoradiogram for LRRK2 autophosphorylation. Reactions were started by the addition of ATP-γ-32P (MP Biomedicals) at the final concentration of 50 μM (2 Ci/mmol) and were stopped after 15 min by mixing with Laemmli buffer. Stained gels then were dried, exposed to a phosphor imaging screen (Molecular Devices), and scanned by Typhoon 9400 (GE Healthcare). Data are representative of three independent experiments. The images were analyzed by Image J as indicated in Fig. 3*B*.

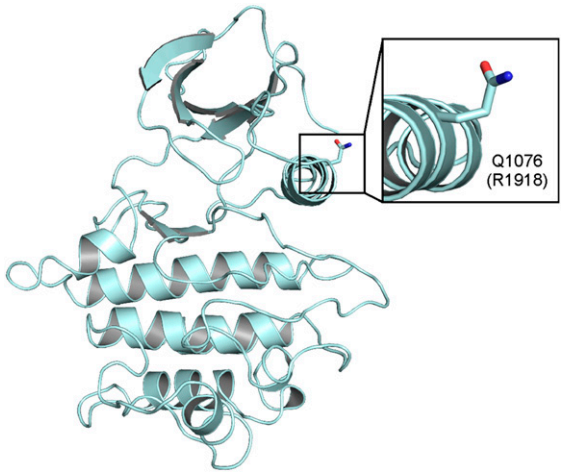

Fig. S3. Ribbon diagram of wild-type Roco4 kinase in the active state. The enlarged view of the αC-helix shows that Q1076 (blue/red) points into the solvent.

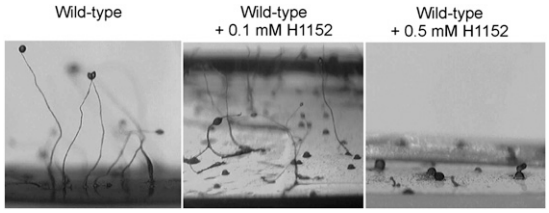

Fig. S4. Side view of the development of wild-type cells in the presence of the indicated concentration of H1152. Cells manifest the typical *roco4*-null phenotype partially in the presence of 0.1 mM H1152 and completely in the presence of 0.5 mM H1152.

Table S1. Data collection and refinement statistics (molecular replacement)

Crystal	Active	Inactive	G1179S	L1180T	H1152
Data collection	Native	Native	Native	Native	Native
Space group	P4(3)2(1)2	P4(3)2(1)2	P4(3)2(1)2	P4(3)2(1)2	P4(3)2(1)2
Cell dimensions					
A, *b*, *c* (Å)	42.7, 42.7, 339.5	42.8, 42.8, 348.2	42.2, 42.2, 332.8	42.3,42.3, 332.6	43.2, 43.2, 352.520
α,β,γ (°)	90.0, 90.0, 90.0	90.0, 90.0, 90.0	90.0, 90.0, 90.0	90.0, 90.0, 90.0	90.0, 90.0, 90.0
Resolution (Å)*	19.1 (1.8)	19.2 (2.0)	41.9 (2.0)	41.9 (2.3)	42.0 (2.3)
R_{sym} or R_{merge}	0.07 (0.46)	0.08 (0.37)	0.10 (0.40)	0.12 (0.38)	0.09 (0.25)
$I/\sigma I$	16.45 (3.09)	13.48 (3.17)	11.65 (3.18	12.09 (3.40)	14.70 (5.22)
Completeness (%)	99,9 (100)	100 (100)	100 (100)	100 (100)	99.9 (100)
Redundancy	9.6 (9.8)	10.1 (10.0)	12.1 (13.0)	11.8 (12.5)	6.9 (7.0)
Refinement					
Resolution (Å)	1.8	2.0	2.0	2.3	2.3
No. reflections	29,252	23,383	19,611	13,871	16,137
$R_{work/}$ R_{free}	0.19/0.24	0.23/0.26	0.26/0.29	0.25/0.29	0.19/0.23
No. atoms					
Protein	2,208	2,113	2,219	2,207	2,160
Ligand/ion	31	—	46	31	44
Water	211	62	96	165	54
B-factors					
Protein	29.9	43.6	26.1	32.8	45.6
Ligand/ion	55.3	—	24.6	70.8	70.3
Water	31.5	30.2	25.7	34.1	31.2
R.m.s deviations					
Bond lengths (Å)	0.027	0.007	0.006	0.006	0.024
Bond angles (°)	2.246	0.987	0.956	0.958	1.953

*Highest-resolution shell is shown in parentheses.